Exploring Spatial Focusing Effect for Spectrum Sharing and Network Association

Chunxiao Jiang, *Senior Member, IEEE*, Beibei Wang, *Senior Member, IEEE*, Yi Han, *Member, IEEE*, Zhung-Han Wu, *Member, IEEE*, and K. J. Ray Liu, *Fellow, IEEE*

***Abstract*— Next-generation wireless networks are expected to support an exponentially increasing number of users and demands of data, which all rely on the essential media: spectrum. Spectrum sharing among heterogeneous networks is a fundamental issue that determines network performance. Previous works have focused on a "dynamic spectrum access" mode associated with the cognitive radio technology. These works all focused on the discovery of available spectrum resource either in the time domain or in the frequency domain, i.e., by separating different users' transmission. To initiate a new paradigm of spectrum sharing, the unique characteristics of the technologies should be utilized in the next-generation networks. The 5G networks are featured either by wide bandwidth like mm-wave systems, or by large-scale antennas like massive MIMO. Those two trends can lead to a common phenomenon: the spatial focusing effect. Based on this focusing effect, we propose a general spatial spectrum sharing framework that enables concurrent multi-users spectrum sharing without the requirement of orthogonal resource allocation. Moreover, we design two general network association protocols either in a centralized manner or in a distributed manner. Simulation results show that both the time reversal wideband and the massive MIMO system can achieve high throughput performance with the spatial spectrum sharing scheme.**

***Index Terms*— Spectrum sharing, spatial focusing, massive MIMO, time reversal, network association.**

I. Introduction

SPECTRUM sharing has been continuously attracting the attention of the research community. It evolved from the original simple division multiple access schemes to some recent progress towards the development of dynamic spectrum access (DSA) in cognitive radio (CR) [1]. Fundamentally, those technologies are all about the discovery of white space in spectrum either in the time domain, e.g., the so-called underlay sharing and overlay sharing [2]; or in the frequency domain, e.g., the so-called in-band sharing and out-of-band sharing [3]; or in the spatial domain, i.e., the geo-location databases [4]. When it comes to the emerging 5G era, it is expected to rely on new characteristics of the 5G systems, such as the massive MIMO (multiple-input-multiple-output) effect, that can be utilized for designing a new generation of spectrum sharing solutions.

In this paper, we focus on a special phenomenon in 5G networks: the spatial focusing effect [5], [6], especially waveforming (such as the time-reversal waveform) is employed when the bandwidth becomes wider and wider as in mm-wave or beamforming (such as maximum-ratio combining beamforming) when the scale of antennas becomes larger and larger as in massive MIMO. The spatial focusing effect means that the intended reception signal can be concentrated at the intended location of the receiver with little energy leakage to the others. This focusing effect is fundamentally due to the decreased correlation between the channel states of two different locations. On one hand, the massive number of antennas can create the channel state information with large dimension for each location. By utilizing a matched filter based precoder or equalizer, the signal energy can concentrate on a corresponding location [7]. On the other hand, the wide bandwidth can help reveal multiple paths in a rich scattering environment, e.g., the scenarios of indoor or dense metropolis. By utilizing the time reversal (TR) technology [5], [8], the signal energy can also concentrate on an intended location, generating the spatial focusing effect. In TR communications, when transceiver A wants to transmit information to transceiver B, transceiver B first has to send a delta-like pilot pulse that propagates through a scattering and multi-path environment and the signals are received by transceiver A; then, transceiver A simply transmits the time-reversed signals back through the same channel to transceiver B. As a matter of fact, those multi-paths can be regarded as virtual antennas and the TR processing can be regarded as cooperatively controlling those antennas, which can realize the similar effect as massive MIMO [6].

This common spatial focusing phenomenon creates a tunnelling effect for each user at his/her own location, such that the interference among different users are rather weak. Thus, multiple users can concurrently conduct data transmission upon the entire spectrum by utilizing their corresponding channel state information as a unique signature. In essence, their locations have ideally separated them in the spatial domain and each different location is a spatial "white space". Therefore, this emerging spatial focusing effect enables us

Manuscript received August 7, 2016; revised January 3, 2017 and March 4, 2017; accepted April 10, 2017. Date of publication April 19, 2017; date of current version July 10, 2017. The associate editor coordinating the review of this paper and approving it for publication was R. Zheng. *(Corresponding author: Chunxiao Jiang.)*

C. Jiang was with the University of Maryland at College Park, College Park, MD 20742 USA and also with Origin Wireless, Inc., Greenbelt, MD 20770 USA. He is now with the Tsinghua Space Center, Tsinghua University, Beijing 100084, China (e-mail: jchx@tsinghua.edu.cn).

B. Wang, Y. Han, Z.-H. Wu, and K. J. R. Liu are with Origin Wireless, Inc., Greenbelt, MD 20770 USA, and also with the Department of Electrical and Computer Engineering, University of Maryland at College Park, College Park, MD 20742 USA (e-mail: bebewang@umd.edu; zhwu@umd.edu; kjrliug@umd.edu; yi.han@originwireless.net).

Color versions of one or more of the figures in this paper are available online at http://ieeexplore.ieee.org.

Digital Object Identifier 10.1109/TWC.2017.2694832

to develop a general spatial spectrum sharing scheme, which allows the reuse of the entire spectrum, instead of separating users either in time domain or in the spectrum domain like the traditional dynamic spectrum access technology. Note that the traditional so-called spatial domain dynamic spectrum access based on geo-location databases is different from the spatial spectrum sharing proposed in this paper. The functionality of the geo-location databases is to record the spatial white-space locations that allow secondary users to utilize without harmful interference to the primary users. In contrast, our spatial spectrum sharing means every location can be regarded as a white space and primary/secondary users can concurrently share the entire spectrum all the time wherever they are located. The major challenge of the spatial spectrum sharing lies in the waveforming design in TR or the beamforming design in massive MIMO, according to some specific criterions. In this paper, instead of focusing on the design of waveformer or beamformer, we are more interested in the spectrum sharing performance analysis given a specific waveformer or beamformer.

The contributions of this paper can be summarized as follows.

1) We leverage the spatial focusing to develop the concept of spatial white space. It can be interpreted as a spatial radio resonance phenomenon at a specific location. This phenomenon has been observed in both TR wideband systems and massive MIMO systems.
2) We propose a general spatial spectrum sharing framework for 5G networks including both TR wideband systems and massive MIMO systems, which supports massive users to concurrently share the entire spectrum all the time.
3) We theoretically analyze the closed-form signal-to-interference-plus-noise ratio (SINR) expressions for both TR wideband and massive MIMO systems. It is found that the SINR of both systems share the same expression under the equal power allocation scenario.
4) Based on the SINR performance analysis, we propose two general network association protocols either in a centralized manner or a distributed manner, which are applicable for both TR wideband systems and massive MIMO systems due to exactly the same formulation of the SINR performance.

The remaining of this paper is organized as follows. Section II summarizes the related works, and Section III presents the system models for both TR wideband systems and massive MIMO systems. Based on the system models, we show the spatial focusing characteristic of both systems in Section IV. Then, a thorough SINR performance analysis is conducted for both systems in Section V, which leads to two general network association protocols design in Section VI. Simulation results are shown in Section VII and conclusions are drawn in Section VIII.

II. Related Works

In the literature, spectrum sharing for 5G networks has been preliminarily studied in [9]–[14], where the researchers have attempted to incorporate a range of new emerging technologies to the spectrum sharing issue. The "software defined network" (SDN) technology was applied to the heterogeneous networks (HetNets) spectrum sharing in [9], where the key contribution is the concept of harmonized SDN-enabled framework, relying on distributed input reporting on spectrum availabilities instead of the traditional spectrum-sensing based approach [15], [16]. Meanwhile, the prediction of the spectrum usage was introduced in [10], with the key contribution of exploring the fundamental limits of predictability of spectrum usage patterns in TV bands, ISM bands, cellular bands, and so on. Another prediction of primary users' moving trajectory was proposed in [11], which initiatively transformed the spectrum sensing problem into a primary users' location tracking problem. Moreover, Mitola, contributed a concept of public-private spectrum sharing in [12], as well as an architecture separating the function between control and data. Similarly, Ng *et al.* proposed to simultaneously utilize licensed and unlicensed bands to improve the energy efficiency and formulated a convex optimization formulation by maximizing the energy efficiency in [13]. Apart from the perspectives of users, the authors in [14] designed a coordination protocol among a set of operators having similar rights for accessing spectrum based on reciprocity modeling from the perspectives of operators.

The medium access control (MAC) layer design for 5G spectrum access has also attracted researchers' attentions. An earlier work in [17] highlighted that due to the small carrier wavelength in mm-wave (millimeter wave), narrow beams are essential for overcoming higher path loss, which can alleviate the inter-user interference, yet making the carrier sensing infeasible and thus leading to severe collision problem. The collision probability analysis of mm-wave systems was a main contribution in [17]. Similarly, based on the narrow beam characteristics of mm-wave networks, the authors in [18] contributed a two-step synchronization and initial access scheme through directional cell search. Meanwhile, in [19], the coverage and rate analysis in mm-wave system was derived under a stochastic geometry framework with the knowledge of antenna beamforming pattern and base station density. Recently, a user association scheme for load balancing and fairness in mm-wave systems was proposed in [20] based on a convex optimization formulation, and a scheduling algorithm for multi-hop mm-wave system was designed in [21] by modeling three kinds of interference. The scenario of heterogeneous networks equipped with massive MIMO was considered in [22], where the authors contributed two algorithms including a cell association algorithm and an antenna allocation algorithm based on the evolutionary game model, which belongs to the game theoretical cognitive radio networks [23], [24]. Another three user association schemes for massive MIMO networks in [25]–[27] were all based on convex optimization model, where the sum rate of the network was optimized under the constraints of fairness and limited resources.

As one can see from the aforementioned works [10]–[27], the researchers have attempted to re-treat the spectrum sharing problem either by incorporating some new technologies like the SDN and the predictions, or by taking into account some unique characteristics of 5G networks like the narrow beams

in mm-wave and the large-scale antenna selection in massive MIMO. Different from those existing works, we focus on the spatial focusing effect [5], [6] in this paper, especially waveforming is employed when the bandwidth becomes wider and wider as in mm-wave or beamforming when the scale of antennas becomes larger and larger as in massive MIMO.

III. System Models

In this section, we introduce the system and channel models for both TR wideband and massive MIMO systems. Basically, the TR wideband system is featured with a single antenna where each antenna is associated with a wide bandwidth up to hundreds or even thousands of MHz; while the massive MIMO system is featured with a large number of antennas but the bandwidth of each antenna is limited to 20-40 MHz. The different bandwidth settings lead to different channel models for these two systems. Generally, in this paper, we consider a multi-user downlink network over non-line of sight multi-path Rayleigh fading channels. Note that in essence, the spatial focusing effect described in this paper is due to the multi-path channel, which provides ample degrees of freedom. Therefore, the channel model has no impact on the results in this paper, e.g. Winner II channel model.

A. Time Reversal Wideband System

1) Downlink Transmission: In the TR wideband system, suppose there are M base stations (BSs) where each BS is equipped with a single antenna, and N user equipments (UEs) where each UE is with a single antenna. The TR wideband downlink system consists of two phases: the channel probing phase and the downlink transmission phase [28]. The channel probing phase is for enabling each BS to obtain the CIRs of each link between it and the associated UEs. This can be done by the following procedure, the N UEs first sequentially transmit an impulse Dirac δ-function signal to the BSs, and the BSs then record and store the CIRs for the transmission phase. In practice, the sequential probing manner can be substituted by designing simultaneous orthogonal probing sequence and the impulse δ-function signal can be a modified raise-cosine signal. After this channel probing phase, the BSs start the transmission phase. As shown in Fig. 1-(a), for the j-th UE, let us denote A_j as the BS that the UE is associating with and denote $\mathcal{N}_{A_j}$ as the current set of UEs that are associating with BS A_j besides the j-th UE. The intended message for those UEs belonging to $\mathcal{N}_{A_j}$ can be represented by $\{X_j, X_{j'\in\mathcal{N}_{A_j}}\}$, where each of the sequence of information symbols X_j or $X_{j'}$ are independent complex random variables with zero mean and $\mathbb{E}\left[|X_{j,j'}[k]|^2\right] = 1$. This sequence of message is first up-sampled by the back-off factor D into $\{X_j^{[D]}, X_{j'\in\mathcal{N}_{A_j}}^{[D]}\}$ for the sake of alleviating the inter-symbol interference due to the delay spread. The up-sampled sequence is then convoluted with the signature generated by the CIRs. The signature can be the time reversal waveform which is a time reversed and conjugated version of each CIR, or can be the enhanced time reversal waveform, i.e., sum rate optimization [29], [30], or

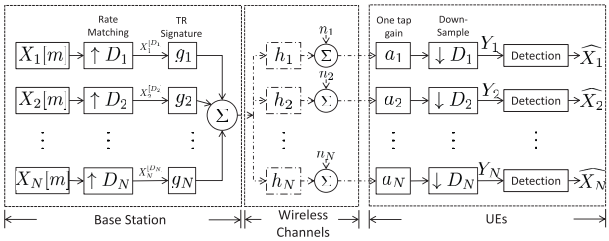

(a) TR wideband system.

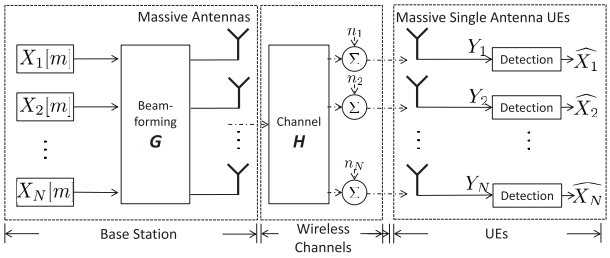

(b) Massive MIMO system.

Fig. 1. System models. (a) TR wideband system. (b) Massive MIMO system.

interference cancelation [31], [32]. After that, all the convoluted messages are added up and transmitted into wireless channels. The transmission power of each BS's antenna is regarded as identical P, and the power allocation for the j-th TD can be denoted by $P_{A_j,j}$, where it should be satisfied that $P_{A_j,j} + \sum_{j'\in\mathcal{N}_{A_j}} P_{A_j,j'} = P$. In such a case, the transmission signal of BS A_j can be written by

$$S_{A_j}[k] = \sqrt{P_{A_j,j}}\left(X_j^{[D]} * g_{A_j,j}\right)[k] + \sum_{j'\in\mathcal{N}_{A_j}} \sqrt{P_{A_j,j'}}\left(X_{j'}^{[D]} * g_{A_j,j'}\right)[k], \quad (1)$$

where $g_{A_j,j}^{\phi}$ is the signature between the ϕ-th antenna of BS A_j and the j-th UE. Note that (1) is based on the assumption that the uplink and downlink channels are reciprocal.

2) Channel Model: The TR system is considered to be a single-carrier system with non-orthogonal resource allocation. Since each antenna is considered to operate upon hundreds of MHz bandwidth, multiple taps channel can be considered as follows. The channel between the i-th BS and the j-th UE can be modeled by the large scale fading incurred by the distance attenuation combined the small scale fading incurred by the multi-path environment. The small scale fading, denoted by $\mathbf{h}_{i,j}$, can be written by

$$\mathbf{h}_{i,j} = \left[h_{i,j}[0], h_{i,j}[1], \ldots, h_{i,j}[L-1]\right], \quad (2)$$

where $h_{i,j}[k]$ represents the k-th tap of the channel impulse response (CIR) with length L and can be written by

$$h_{i,j}[k] = \sum_{l=0}^{L-1} h_{i,j}^{l}\delta[k-l], \quad (3)$$

with $\delta[\cdot]$ as the Dirac delta function. In this paper, we consider a rich-scattering environment, in which due to the spatial heterogeneity and the rich multi-paths, the CIRs of different UEs in different locations are assumed to be uncorrelated.

3) Downlink Reception: For the receiver side of the TR wideband system, the received signal of the j-th UE can be represented as follows

$$Y_j^{[D]}[k] = \sum_{i=1}^{M} d_{i,j}^{-\alpha/2} \left(S_i * h_{i,j}\right)[k] + n_j[k], \tag{4}$$

where $d_{i,j}$ represents the distance between the i-th BS and the j-th UE, α is the path loss coefficient, $d_{i,j}^{-\alpha/2}$ represents the aforementioned large scale fading incurred by the distance attenuation, $h_{i,j}$ represents the small scale fading between the i-th BS and the j-th UE, and n_j represents the additive white Gaussian noise with zero mean and variance σ^2.

B. Massive MIMO System

1) Downlink Transmission: In the massive MIMO system, suppose there are M BSs each associated with a massive number of antennas Φ, and N UEs each with a single antenna with $1 \ll N \ll \Phi$. Similar to the TR wideband system, the massive antenna system also includes two phase: the channel state information (CSI) acquisition phase using an uplink pilot and the data transmission phase [33]. Here, the CSI is assumed to be perfectly known by the BSs so that they can perform beamforming to support multiple UEs' data transmission. As shown in Fig. 1-(b), let us denote the beamforming matrix of the i-th BS as $\mathbf{G}_i = \{\mathbf{g}_{i,1}, \mathbf{g}_{i,2}, \ldots, \mathbf{g}_{i,|\mathcal{N}_i|}\}$, where $\mathbf{G}_i \in \mathbb{C}^{\Phi \times |\mathcal{N}_i|}$, $\mathbf{g}_{i,j} \in \mathbb{C}^{\Phi \times 1}$, and $\mathcal{N}_i$ represents the set of UEs that associate with the i-th BS and the number of UEs in $\mathcal{N}_i$ is denoted as $|\mathcal{N}_i|$. Note that the beamforming matrix can be MRC (maximal-ratio combining), ZF (zero-forcing) [34]–[36], or MMSE (minimum mean square error) [37], [38]. Suppose $\mathbf{s}_i = [s_{i,1}, s_{i,2}, \ldots, s_{i,|\mathcal{N}_i|}]^{\mathrm{T}}$ is the transmit symbols of the i-th BS with length determined by the number of UEs that associate with it, where $\mathbf{s}_i \in \mathbb{C}^{|\mathcal{N}_i| \times 1}$ and $\mathbb{E}(\mathbf{s}_i \mathbf{s}_i^*) = \mathbf{I}$.

2) Channel Model: The bandwidth of each antenna is assumed to be regular wideband as 20-40 MHz, where OFDM is employed to provide a group of single-tap sub-carriers. For the simplicity of expression, we assume flat fading for each antenna [33], and thus denote the small scale fading between the i-th BS and its associated UEs as follows:

$$\mathbf{H}_i = \{\mathbf{h}_{i,1}^{\mathrm{T}}, \mathbf{h}_{i,2}^{\mathrm{T}}, \ldots, \mathbf{h}_{i,|\mathcal{N}_i|}^{\mathrm{T}}\}, \tag{5}$$

where $\cdot^{\mathrm{T}}$ represents the transpose operation. In such a case, we have $\mathbf{H}_i \in \mathbb{C}^{\Phi \times |\mathcal{N}_i|}$ where $\mathbb{C}$ represents the complex domain, i.e., $\mathbf{h}_{i,j} \in \mathbb{C}^{1 \times \Phi}$ is the small-scale fading channel between the i-th BS and the j-th UE in $\mathcal{N}_i$.

3) Downlink Reception: The received signal of the j-th TD can be expressed by

$$Y_j = \sum_{i=1}^{M} \sqrt{P} d_{i,j}^{-\alpha/2} \mathbf{h}_{i,j} \mathbf{G}_i \mathbf{s}_i + n_j, \tag{6}$$

where P represents the transmission power of each antenna, $d_{i,j}$ represents the distance between the i-th BS and the j-th UE, α is the path loss coefficient, $d_{i,j}^{-\alpha/2}$ represents the large scale attenuation, and n_j represents the additive white Gaussian noise with zero mean and variance σ^2. Note that the inter-cell interference has been taken into account in (6), since the summation means the received signal from all other BSs besides the BS that the j-th TD associates with. In order to achieve a similar setting as in the aforementioned TR wideband system, it is also assumed a one-tap receiver in the massive MIMO system.

IV. Spatial Focusing Effect

In this section, we introduce a special phenomenon in both TR wideband and massive MIMO systems: the spatial focusing effect. This focusing effect means that the signal for an intended location can concentrate only at that specific location with only little energy leakage to other locations, by waveforming (e.g., utilizing an appropriate waveform) based on the channel state information of that specific location. Based on this spatial focusing effect, the multi-users' concurrent data transmission can be readily achieved [28] since the interference among UEs can be alleviated to a large extent due to the energy concentration, which enables the entire spectrum sharing among primary users and secondary users simultaneously. Note that the spatial focusing of TR communications was firstly mentioned in [8], while later the spatial focusing effect of massive MIMO was mentioned in [7]. Nevertheless, how to leverage the spatial focusing effect to the spectrum sharing has not been investigated in those two works. In this paper, our work is pioneer in proposing a spatial spectrum sharing framework, as well as the performance analysis. There are two major challenges: one is the waveforming design for the TR system and the beamforming design for massive MIMO system, and the other is the CSI acquisition when the number of users is relativelh large. In this paper, we will analyze the spectrum sharing performance of the time-reversal waveforming and MRC beamforming, while the CSI acquisition is not the focus.

A. Ray-Tracing Based Simulation

As aforementioned, both TR wideband and massive MIMO systems can exhibit this spatial focusing effect. However, the approaches are different where the TR system relies on a wide bandwidth but the massive MIMO system relies on a large number of antennas. For the TR wideband system in a rich scattering environment with multi-path propagation (e.g., dense city or indoor scenarios), the wide bandwidth can help reveal those multiple paths from the transmitter to each specific location. The wider bandwidth can reveal more multi-paths for each location, and thus can lead to less correlation between every two different locations' channels. Eventually, by utilizing the time-reversed CIR of a specific location as the waveform of this location, the convolution of the waveform and the channel can generate a unique peak at that specific location, with little energy leakage to the neighboring locations. For the massive MIMO system equipped with a large scale of antennas, those antennas can physically create a large dimension of CSI for each location, which also leads to the small correlation among difference locations. Therefore, by utilizing a simple matched filter precoder based on the CSI of

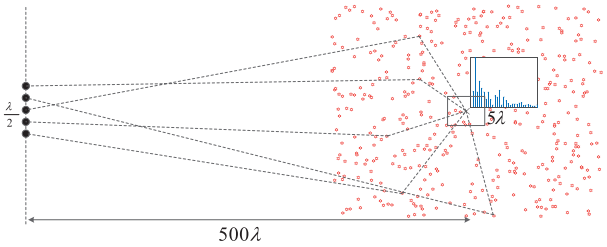

Fig. 2. Simulation setup for validating spatial focusing effect.

a specific location, the signal energy can be spatially focused at that specific location.

To validate this spatial focusing effect, we construct a ray-tracing based simulation in a discrete scattering environment. As shown in Fig. 2, a total number of 400 effective scatters are distributed randomly in a square area with dimension $200\lambda \times 200\lambda$, where λ is the wavelength corresponding to the carrier frequency. In such a case, the wireless channel can be represented as a sum of multi-paths using the classical ray-tracing method. Without loss of generality, we adopt a single-bounce ray-tracing model in computing the channel impulse responses in both TR wideband and the large scale antenna array systems, where both systems are operated on 5GHz ISM band. The reflection coefficient of each scatter is chosen to be I.I.D. complex random variables with uniform distribution both in amplitude (from 0 to 1) and phase (from 0 to 2π). For the large antenna array system as show in Fig. 2, the antennas are placed in a line facing the scattering area and the interval between each two adjacent antennas is $\lambda/2$. Moreover, the distance between the transmitter and the intended location is chosen to be 500λ for both systems.

In the simulation, for the TR wideband system, it is assumed to be equipped with only a single antenna, and the bandwidth is tuned from 100 MHz to 500 MHz. With a wider bandwidth, more multi-paths can be resolved and thus the CIR have more taps accordingly. By contrast, for the large antenna array system, the number of antennas is adjusted from 20 to 100, while the bandwidth of the system is fixed to be 1 MHz. This narrow-band configuration guarantees that the CIR has a single tap, which is a common assumption in OFDM-based massive MIMO literature [7]. In order to achieve the energy concentration at the intended location, time-reversal mirror precoder and matched filter precoder are applied in TR wideband and large antenna array systems, respectively. As shown in Fig. 2, we consider the field strengths around the intended location with dimension $5\lambda \times 5\lambda$. Fig. 3 shows the simulation results of both systems, where the maximal received signal strength is set to be 0dB for normalization. We can clearly see that for the TR wideband system, the spatial focusing effect can be improved with wider and wider bandwidth. Similarly, for the large antenna array system, the increasing number of antennas can also lead to better spatial focusing effect. Therefore, those simulation results corroborate the existence of spatial focusing phenomenon in future 5G systems when the bandwidth becomes wider as in the mm-Wave system or the number of antennas becomes massive as in the massive

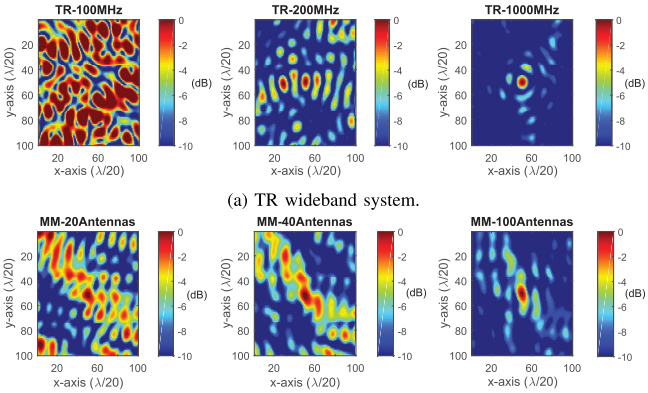

(a) TR wideband system.

(b) Massive MIMO system.

Fig. 3. Spatial focusing effect of both systems. (a) TR wideband system. (b) Massive MIMO system.

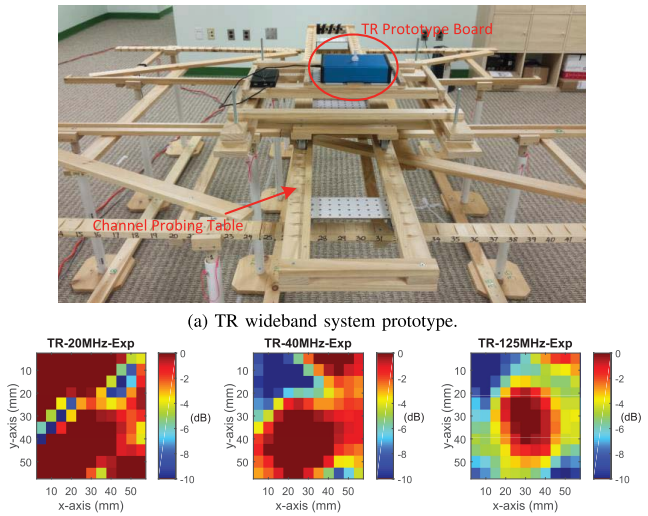

(a) TR wideband system prototype.

(b) Experiment results.

Fig. 4. Spatial focusing effect of TR wideband system prototype. (a) TR wideband system prototype. (b) Experiment results.

MIMO system. Note that in the dynamic scenario, once a user moves out of the spatial focusing spot, the CSI is required to be updated such that the new spatial focusing spot can be established. Therefore, how much users can move in the network is determined by the frequency of CSI updating.

B. Prototype Based Experiment

To further verify the spatial focusing effect, we built a prototype of TR wideband system on a customized software-defined radio (SDR) platform, as shown in Fig. 4-(a). The hardware architecture combines a specific designed radio-frequency board covering the ISM band with 125 MHz bandwidth, a high-speed Ethernet port, and an off-the-shelf user-programmable module board. In this experiment, we measure the CIRs of a square region with dimension 5cm × 5cm on a channel probing table which is located in a typical office environment as shown in Fig. 4. The intended location is chosen to be the center of the measured region and the corresponding normalized field strength is shown in Fig. 4-(b).

We can see that the TR transmission can generate a clear energy focusing around the intended location, even under a not-so-wide bandwidth of 125 MHz. Relying on this spatial focusing effect, the UEs at different locations can be ideally separated, which enables the concurrent data transmission over the entire spectrum.

C. Spatial Spectrum Sharing

As we can see from both the simulation and experiment results, the spatial focusing effect commonly exist either in wideband systems or in large-scale antenna systems. This common spatial focusing phenomenon enables us to find a general spatial spectrum sharing scheme, where multiple users can concurrently conduct data transmission upon the entire spectrum by utilizing their corresponding channel state information as a unique signature, i.e., their locations have ideally separated them in the spatial domain. The spatial spectrum sharing scheme is rather simple that, taking the downlink transmission for an example, all the UEs' signal can be added together and transmitted simultaneously by the BS. The system models illustrated in Fig. 1 have indicated the essence of the spatial spectrum sharing scheme, where for TR wideband system, all UEs' signals are added together after convoluted with their own signatures and the sum of the signals are transmitted simultaneously; and for massive MIMO systems, all UEs' signals are multiplied by the beamforming matrix and then also transmitted simultaneously. Note that the proposed spatial spectrum sharing is independent of the network operators, since every pair of transmitter and receiver is barely interfered by other pairs in the physical layer, whether within the same operator or not. In the next section, we will analyze the performance of such a spatial spectrum sharing scheme.

V. Spatial Spectrum Sharing Performance

Based on the spatial focusing effect, our further contribution in this paper is to theoretically analyze the closed-form signal-to-interference-plus-noise ratio (SINR) expressions for both TR wideband and massive MIMO systems. Moreover, two general network association protocols either in a centralized manner or a distributed manner will be proposed, which are also applicable for both systems. In this section, we evaluate the spatial spectrum sharing performance based on the system models described in the previous sections. Although the spatial focusing effect can help separate multi-users' simultaneous transmission, the non-ideal uncorrelated channels can still lead to minor inference to each other. Hence, we quantify such interference for both systems in this section as well as the effective SINR performance. SINR is a direct quantified metric reflecting the spatial focusing effect, i.e., a higher SINR represents the signal power is more concentrated at the intended receiver. Moreover, SINR is also a direct indicator to the data rate and the system throughput performance, and thus is deduced in detail in this paper. As we will see later, an interesting phenomenon shows that the SINR expression of both TR wideband and massive MIMO systems share the same formulation, which is fundamentally due to the similar spatial focusing effect existing in both systems.

A. Time Reversal Wideband System

Let us consider the multi-user downlink transmission of a TR wideband system. Thanks to the spatial and temporal focusing effect, the signal energy can be concentrated in a single time sample at the location of the intended UE. In such a case, the j-th UE just simply performs a one-tap gain adjustment a_j to the received signal to recover the signal and then down-samples it with the same back-off factor D. Thus, the down-sampled received signal of the j-th UE, denoted by $Y_j[k]$, can be written as follows:

$$Y_j[k] = a_j \sum_{i=1}^{M} \sum_{l=0}^{(2L-2)/D} d_{i,j}^{-\alpha/2} \left(S_i * h_{i,j}\right)[Dl] + a_j n_j[k], \tag{7}$$

where for notational simplicity, we have assumed $L-1$ to be a multiple of back-off factor D. To better understand the received signal $Y_j[k]$, we further re-write it into the following separated formulation, from which the inter-symbol interference (ISI), inter-user interference (IUI), and inter-cell interference (ICI) can be clearly illustrated.

$$\begin{aligned} Y_j[k] = {} & a_j \sum_{\phi=1}^{\Phi_t} \sqrt{P_{A_j,j}} X_j[k] \cdot d_{A_j,j}^{-\alpha/2} \left(h_{A_j,j}^{\phi} * g_{A_j,j}^{\phi}\right)[L-1] \\ & + a_j \sum_{\substack{l=0 \\ l \neq (L-1)/D}}^{(2L-2)/D} \sum_{\phi=1}^{\Phi_t} \sqrt{P_{A_j,j}} X_j[k-l] \cdot d_{A_j,j}^{-\alpha/2} \\ & \times \left(h_{A_j,j}^{\phi} * g_{A_j,j}^{\phi}\right)[Dl] \\ & + a_j \sum_{j' \in \mathcal{N}_{A_j}} \sum_{l=0}^{(2L-2)/D} \sum_{\phi=1}^{\Phi_t} \sqrt{P_{A_j,j'}} X_{j'}[k-l] \cdot d_{A_j,j}^{-\alpha/2} \\ & \times \left(h_{A_j,j}^{\phi} * g_{A_j,j'}^{\phi}\right)[Dl] \\ & + a_j \sum_{j' \notin \mathcal{N}_{A_j}} \sum_{l=0}^{(2L-2)/D} \sum_{\phi=1}^{\Phi_t} \sqrt{P_{A_{j'},j'}} X_{j'}[k-l] \cdot d_{A_{j'},j}^{-\alpha/2} \\ & \times \left(h_{A_{j'},j}^{\phi} * g_{A_{j'},j'}^{\phi}\right)[Dl] \\ & + a_j n_j[k], \end{aligned} \tag{8}$$

where the first term is the intended signal for the j-th UE, the second term is the ISI caused by channel delay spread, the third term is the IUI caused by the UEs that share the same BS with the j-th UE, the fourth term is the ICI from the other non-intended BSs, and the last term is the noise at the receiver. Let us further explain the physical meanings of (8). The signal power is the maximum-power central peak of the channel impulse response (CIR) autocorrelation, which is the total power of all multiple paths. For the interference, the ISI is physically due to the channel delay spread, and is mathematically due to the cross symbols operation of CIR autocorrelation. The IUI is physically due to the power leakage to an unintended user, and is mathematically due to the existence of correlation among different users' CIR as well as the channel delay spread. The ICI is similar to the IUI, which can be interpreted as IUI from other cells.

Here, we employ the definition of effective SINR, which is the ratio of the average signal power to the average interference-and-noise power, as the performance metric. Note that this effective SINR is an approximation of the standard average SINR definition, i.e.,

$$\mathbb{E}_h\left[\frac{P_{\text{SIG}}}{P_{\text{ISI}}+P_{\text{IUI}}+P_{\text{ICI}}+\sigma^2}\right] \simeq \frac{\mathbb{E}_h\left[P_{\text{SIG}}\right]}{\mathbb{E}_h\left[P_{\text{ISI}}\right]+\mathbb{E}_h\left[P_{\text{IUI}}\right]+\mathbb{E}_h\left[P_{\text{ICI}}\right]+\sigma^2}. \quad (11)$$

While the standard average SINR calculation in the left-hand side of (11) is mathematically intractable due to the complicated convolution and integration operations, in this paper we utilize the effective SINR, i.e., right-hand side of (11), to study the performance, which has been widely utilized in the literature [39]–[41]. Specifically, it has shown in [28] that this approximation is relatively accurate by comparing the simulation results and approximated theoretical results. Based on the definition of the effective SINR, we should first calculate the average signal power and average interference power, respectively. Firstly, the expected intended signal power for the j-th UE from (8), denoted by $\mathbb{E}_h\left[P_{\text{SIG}}\right]$, can be calculated by

$$\begin{aligned}\mathbb{E}_h\left[P_{\text{SIG}}\right] &= a_j P_{A_j,j} d_{A_j,j}^{-\alpha}\mathbb{E}_h\left[\left|\left(h_{A_j,j} * g_{A_j,j}\right)[L-1]\right|^2\right] \\ &= a_j P_{A_j,j} d_{A_j,j}^{-\alpha} C_1, \end{aligned} \quad (12)$$

where we use C_1 to represent the expectation of $\left|\left(h_{A_j,j} * g_{A_j,j}\right)[L-1]\right|^2$ over the CIR. Note that the waveform design vector $g_{A_j,j}$ is a function of CIR $h_{A_j,j}$. Similarly, we can have the average ISI $\mathbb{E}_h\left[P_{\text{ISI}}\right]$, and average IUI $\mathbb{E}_h\left[P_{\text{IUI}}\right]$ from (8) as follows:

$$\begin{aligned}&\mathbb{E}_h\left[P_{\text{ISI}}\right] \\ &= a_j P_{A_j,j} d_{A_j,j}^{-\alpha}\mathbb{E}_h\left[\sum_{\substack{l=0\\ l\neq(L-1)/D}}^{(2L-2)/D}\left|\left(h_{A_j,j} * g_{A_j,j}\right)[Dl]\right|^2\right] \\ &= a_j P_{A_j,j} d_{A_j,j}^{-\alpha} C_2, \end{aligned} \quad (13)$$

$$\begin{aligned}&\mathbb{E}_h\left[P_{\text{IUI}}\right] \\ &= a_j \sum_{j'\in\mathcal{N}_{A_j}} P_{A_j,j'} d_{A_j,j}^{-\alpha} \\ &\quad\cdot\mathbb{E}_h\left[\sum_{l=0}^{(2L-2)/D}\left|\left(h_{A_j,j} * g_{A_j,j'}\right)[Dl]\right|^2\right] \\ &= a_j \sum_{j'\in\mathcal{N}_{A_j}} P_{A_j,j'} d_{A_j,j}^{-\alpha} C_3 \\ &= a_j (P - P_{A_j,j}) d_{A_j,j}^{-\alpha} C_3, \end{aligned} \quad (14)$$

where we use C_2 and C_3 to represent the expectations of $\sum_{\substack{l=0\\ l\neq(L-1)/D}}^{(2L-2)/D}\left|\left(h_{A_j,j} * g_{A_j,j}\right)[Dl]\right|^2$ and $\sum_{l=0}^{(2L-2)/D}|\left(h_{A_j,j} * g_{A_j,j'}\right)[Dl]|^2$, respectively. The calculation of the average ICI $\mathbb{E}_h\left[P_{\text{ICI}}\right]$ requires some special transformation. The ICI in the fourth term of (8) was written by the summation of interference from all UEs belonging to all other non-intended BSs. Since the interference from the UEs sharing the same BS can be regarded as a single interference source from that BS, we can re-write the ICI directly by the summation of interference from all other non-intended BSs. Let us denote $\mathcal{N}_i$ as the set of UEs that associate with the i-th BS. Then, the ICI, i.e., the fourth item in (8), can be written by

$$\text{ICI} = a_j \sum_{\substack{i=1\\ i\neq A_j}}^{M}\sum_{j'\in\mathcal{N}_i}\sum_{l=0}^{(2L-2)/D} X_{j'}[k-l]\cdot d_{i,j}^{-\alpha/2}\left(h_{i,j} * g_{i,j'}\right)[Dl]. \quad (15)$$

By taking expectation over the channel, we can have the average ICI as follows

$$\begin{aligned}\mathbb{E}_h\left[P_{\text{ICI}}\right] &= a_j \sum\nolimits_{\substack{i=1\\ i\neq A_j}}^{M}\sum_{j'\in\mathcal{N}_i} P_{i,j'} d_{i,j}^{-\alpha} \\ &\quad\cdot\mathbb{E}_h\left[\sum\nolimits_{l=0}^{(2L-2)/D}\left|\left(h_{i,j} * g_{i,j'}\right)[Dl]\right|^2\right] \\ &= a_j \sum\nolimits_{\substack{i=1\\ i\neq A_j}}^{M} P d_{i,j}^{-\alpha} C_3, \end{aligned} \quad (16)$$

where C_3 is same with that in (14). By substituting (12), (13), (14), and (15) into the right-hand side of (11), we can obtain the effective SINR of the j-th UE, SINR_j, as in (9), as shown at the top of the next page. Note that (9) is a general expression of the effective SINR evaluation in the TR wideband system. In the following, some special cases will be considered to reveal more characteristics.

Firstly, let us suppose equal power allocation scenario, i.e. the power for each UE belonging to the BS i should be $\frac{P}{|\mathcal{N}_i|}$. In such a case, we can simplify the SINR expression in (9) as in (10), as shown at the top of the next page, where for simplicity, we define the parameters ξ_1, ξ_2 and ξ_3 as follows:

$$\xi_1 = C_1, \quad \xi_2 = C_2 - C_3, \quad \xi_3 = \sum_{i=1}^{M} d_{i,j}^{-\alpha} C_3 + \sigma_j^2/P. \quad (17)$$

Secondly, let us consider the time reversal waveform, i.e.,

$$g_{i,j}[k] = \frac{h_{i,j}^*[L-1-k]}{\sqrt{\mathbb{E}\left[\sum_{l=0}^{L-1}\left|h_{i,j}[l]\right|^2\right]}}, \quad (18)$$

which is the normalized (by the average channel gain) complex conjugate of time reversed $\{h_{i,j}^*[k]\}$. This time reversal waveform can provide with the maximum reception power at the intended symbol, since the first term in (8) corresponds to the maximum-power central peak of the autocorrelation function, i.e.,

$$\left(h_{A_j,j} * g_{A_j,j}\right)[L-1] = \frac{\sum_{l=0}^{L-1}\left|h_{i,j}^*[l]\right|^2}{\sqrt{\mathbb{E}\left[\sum_{l=0}^{L-1}\left|h_{i,j}[l]\right|^2\right]}}. \quad (19)$$

Furthermore, by considering the exponential-decay multi-path channel model, we have

$$\mathbb{E}\left[\left|h_{i,j}[k]\right|^2\right] = e^{-\frac{kT_s}{\sigma_T}}, \quad 0\le k\le L-1, \quad (20)$$

$$\mathbb{E}\left[\left|h_{i,j}[k]\right|^4\right] = 2\left(\mathbb{E}\left[\left|h_{i,j}[k]\right|^2\right]\right)^2 = 2e^{-2\frac{kT_s}{\sigma_T}}, \quad (21)$$

where the k-th tap between the i-th BS and the j-th UE, $h_{i,j}[k]$, is assumed to be a circular symmetric complex

$$\begin{aligned}\mathrm{SINR}_j &= \frac{a_j P_{A_j,j} d_{A_j,j}^{-\alpha} C_1}{a_j P_{A_j,j} d_{A_j,j}^{-\alpha} C_2 + a_j (P - P_{A_j,j}) d_{A_j,j}^{-\alpha} C_3 + a_j \sum_{\substack{i=1 \\ i\neq A_j}}^{M} P d_{i,j}^{-\alpha} C_3 + a_j \sigma_j^2} \\ &= \frac{P_{A_j,j} d_{A_j,j}^{-\alpha} C_1}{P_{A_j,j} d_{A_j,j}^{-\alpha} C_2 - P_{A_j,j} d_{A_j,j}^{-\alpha} C_3 + \sum_{i=1}^{M} P d_{i,j}^{-\alpha} C_3 + \sigma_j^2}. \end{aligned} \tag{9}$$

$$\begin{aligned}\mathrm{SINR}_j &= \frac{\frac{P}{\left|\mathcal{N}_{A_j}\right|+1} d_{A_j,j}^{-\alpha} C_1}{\frac{P}{\left|\mathcal{N}_{A_j}\right|+1} d_{A_j,j}^{-\alpha} C_2 + \frac{\left|\mathcal{N}_{A_j}\right| P}{\left|\mathcal{N}_{A_j}\right|+1} d_{A_j,j}^{-\alpha} C_3 + \sum_{\substack{i=1 \\ i\neq A_j}}^{M} P d_{i,j}^{-\alpha} C_3 + \sigma_j^2} \\ &= \frac{C_1}{C_2 - C_3 + \left(\left|\mathcal{N}_{A_j}\right| + 1\right) d_{A_j,j}^{\alpha} \left(\sum_{i=1}^{M} d_{i,j}^{-\alpha} C_3 + \sigma_j^2 / P\right)} = \frac{\xi_1}{\xi_2 + \xi_3 \left(\left|\mathcal{N}_{A_j}\right| + 1\right) d_{A_j,j}^{\alpha}}, \end{aligned} \tag{10}$$

Gaussian random variable with zero mean and aforementioned variance, T_s is the sampling period of the system such that $1/T_s$ equals to the system bandwidth B, and δ_T is the root mean square delay spread of the channel. Based on this exponential-decay multi-path channel model, we can calculate the closed-form expressions for C_1, C_2 and C_3, and in turn, the expressions of ξ_1, ξ_2 and ξ_3 as follows:

$$\xi_1 = \frac{1 + e^{-\frac{LT_s}{\sigma_T}}}{1 + e^{-\frac{T_s}{\sigma_T}}} + \frac{1 - e^{-\frac{LT_s}{\sigma_T}}}{1 - e^{-\frac{T_s}{\sigma_T}}}, \tag{22}$$

$$\begin{aligned}\xi_2 = {} & 2 \frac{e^{-\frac{T_s}{\sigma_T}} \left(1 - e^{-\frac{(L-2+D)T_s}{\sigma_T}}\right)}{\left(1 - e^{-\frac{DT_s}{\sigma_T}}\right)\left(1 + e^{-\frac{T_s}{\sigma_T}}\right)} \\ & - \frac{\left(1+e^{-\frac{DT_s}{\sigma_T}}\right)\left(1+e^{-\frac{2LT_s}{\sigma_T}}\right) - 2e^{-\frac{(L+1)T_s}{\sigma_T}}\left(1+e^{-\frac{(D-2)T_s}{\sigma_T}}\right)}{\left(1 - e^{-\frac{DT_s}{\sigma_T}}\right)\left(1 + e^{-\frac{T_s}{\sigma_T}}\right)\left(1 - e^{-\frac{LT_s}{\sigma_T}}\right)}, \end{aligned} \tag{23}$$

$$\begin{aligned}\xi_3 = {} & \sigma_j^2 / P + \sum_{i=1}^{M} d_{i,j}^{-\alpha} \\ & \cdot \frac{\left(1+e^{-\frac{DT_s}{\sigma_T}}\right)\left(1+e^{-\frac{2LT_s}{\sigma_T}}\right) - 2e^{-\frac{(L+1)T_s}{\sigma_T}}\left(1+e^{-\frac{(D-2)T_s}{\sigma_T}}\right)}{\left(1 - e^{-\frac{DT_s}{\sigma_T}}\right)\left(1 + e^{-\frac{T_s}{\sigma_T}}\right)\left(1 - e^{-\frac{LT_s}{\sigma_T}}\right)}. \end{aligned} \tag{24}$$

Combining (10) and (21)–(23), we have obtained the SINR evaluation of the TR wideband system. In the next subsection, we will analyze the SINR of the massive MIMO system, where it will be seen that the SINR of both systems share exactly the same expression.

B. Massive MIMO System

Let us consider the multi-user downlink transmission of a massive MIMO system. Since the BSs have performed beamforming based on the CSI, the UE can simply do the one-tap detection to receive the signal. Similar to the TR wideband system, the received signal of the j-th UE can be formulated by the summation of the intended signal, IUI and ICI, as follows:

$$\begin{aligned} y_j &= \sum_{i=1}^{M} \sqrt{P} d_{i,j}^{-\alpha/2} \mathbf{h}_{i,j} \mathbf{G}_i \mathbf{s}_i + n_j \\ &= \sqrt{P_{A_j,j}} d_{A_j,j}^{-\alpha/2} \mathbf{h}_{A_j,j} \mathbf{g}_{A_j,j} s_{A_j,j} \\ &\quad + \sum_{j' \in \mathcal{N}_{A_j}} \sqrt{P_{A_j,j'}} d_{A_j,j}^{-\alpha/2} \mathbf{h}_{A_j,j} \mathbf{g}_{A_j,j'} s_{A_j,j'} \\ &\quad + \sum_{\substack{i=1 \\ i\neq A_j}}^{M} \sqrt{P} d_{i,j}^{-\alpha/2} \mathbf{h}_{i,j} \mathbf{G}_i \mathbf{s}_i + \ n_j, \end{aligned} \tag{25}$$

where A_j denotes the BS that the j-th TD will associate with, $\mathbf{h}_{A_j,j}$ denotes the CSI between the BS and the j-th UE, $s_{A_j,j}$ denotes the intended symbol for the j-th UE, $\mathbf{g}_{A_j,j}$ denotes the beamforming vector for the j-th UE, $\mathcal{N}_{A_j}$ denotes the current set of TDs that also associate BS A_j besides the j-th UE, and n_j represents the noise. In the last equality of (24), the first term is the intended signal for the j-th UE, while the second term is the IUI and the third term is the ICI for the j-th UE. Similarly, the physical meanings of the SINR of massive MIMO systems can be interpreted as follows. The signal power represents the intended symbols from all antennas. Since the OFDM technique is commonly adopted in the MIMO systems, the ISI can be neglected in the narrow-band subcarrier. While the IUI and ICI still exist, which are due to the non-ideal un-correlated assumption among difference users' channels. In such a case, we can write the expectation of the j-th UE's signal power and IUI power as follows:

$$\begin{aligned} \mathbb{E}_h\left[P_{\mathrm{SIG}}\right] &= P_{A_j,j} d_{A_j,j}^{-\alpha} \mathbb{E}_h\left[\left|\mathbf{h}_{A_j,j} \mathbf{g}_{A_j,j}\right|^2\right] \\ &= P_{A_j,j} d_{A_j,j}^{-\alpha} C_1', \end{aligned} \tag{26}$$

$$\begin{aligned} \mathbb{E}_h\left[P_{\mathrm{IUI}}\right] &= \sum_{j' \in \mathcal{N}_{A_j}} P_{A_j,j'} d_{A_j,j}^{-\alpha} \mathbb{E}_h\left[\left|\mathbf{h}_{A_j,j} \mathbf{g}_{A_j,j'}\right|^2\right] \\ &= \sum_{j' \in \mathcal{N}_{A_j}} P_{A_j,j'} d_{A_j,j}^{-\alpha} C_2' = (P - P_{A_j,j}) d_{A_j,j}^{-\alpha} C_2', \end{aligned} \tag{27}$$

where we use constants C_1' and C_2' to represent the expectations of $\left|\mathbf{h}_{A_j,j}\mathbf{g}_{A_j,j}\right|^2$ and $\left|\mathbf{h}_{A_j,j}\mathbf{g}_{A_j,j'}\right|^2$, respectively. For the ICI, it can be re-written by

$$\begin{aligned}\text{ICI} &= \sum_{\substack{i=1\\ i\neq A_j}}^{M} \sqrt{P} d_{i,j}^{-\alpha/2} \mathbf{h}_{i,j}\mathbf{G}_i\mathbf{s}_i \\ &= \sum_{\substack{i=1\\ i\neq A_j}}^{M} \sum_{j'\in\mathcal{N}_i} \sqrt{P_{i,j'}} d_{i,j}^{-\alpha/2} \mathbf{h}_{i,j}\mathbf{g}_{i,j'}s_{i,j'}, \end{aligned} \tag{28}$$

and then, we have the power of ICI as follows

$$\begin{aligned}\mathbb{E}_h\left[P_{\text{ICI}}\right] &= \sum_{\substack{i=1\\ i\neq A_j}}^{M} \sum_{j'\in\mathcal{N}_i} P_{i,j'} d_{i,j}^{-\alpha} \mathbb{E}_h\left[\left|\mathbf{h}_{i,j}\mathbf{g}_{i,j'}\right|^2\right] \\ &= \sum_{\substack{i=1\\ i\neq A_j}}^{M} P d_{i,j}^{-\alpha} C_2'. \end{aligned} \tag{29}$$

By integrating (24), (26), and (27) together, we can obtain the effective SINR as follows:

$$\begin{aligned}\text{SINR}_j &= \frac{P_{A_j,j} d_{A_j,j}^{-\alpha} C_1'}{(P - P_{A_j,j}) d_{A_j,j}^{-\alpha} C_2' + \sum_{\substack{i=1\\ i\neq A_j}}^{M} P d_{i,j}^{-\alpha} C_2'} \\ &= \frac{P_{A_j,j} d_{A_j,j}^{-\alpha} C_1'}{-P_{A_j,j} d_{A_j,j}^{-\alpha} C_2' + \sum_{i=1}^{M} P d_{i,j}^{-\alpha} C_2' + \sigma_j^2}. \end{aligned} \tag{30}$$

We can see that, the SINR of both TR wideband and massive MIMO systems are quite similar to each other, while the only difference is that there is no ISI in massive MIMO system due to the single-tap channel assumption, i.e., OFDM operation. In the following, we will see that the SINR of both systems share exactly the same expression under some special scenarios.

Similar to the analysis of the TR wideband system, let us also consider the equal power allocation scenario for the massive MIMO system. Then, we can have $P_{i,j} = P/|\mathcal{N}_i|$, and the following derivations

$$\begin{aligned}\text{SINR}_j &= \frac{\frac{P}{\left|\mathcal{N}_{A_j}\right|+1} d_{A_j,j}^{-\alpha} C_1'}{-\frac{P}{\left|\mathcal{N}_{A_j}\right|+1} d_{A_j,j}^{-\alpha} C_2' + \sum_{i=1}^{M} P d_{i,j}^{-\alpha} C_2' + \sigma_j^2} \\ &= \frac{C_1'}{-C_2' + \left(\left|\mathcal{N}_{A_j}\right|+1\right) d_{A_j,j}^{\alpha} \left(\sum_{i=1}^{M} d_{i,j}^{-\alpha} C_2' + \sigma_j^2/P\right)} \\ &= \frac{\xi_1'}{\xi_2' + \xi_3' \left(\left|\mathcal{N}_{A_j}\right|+1\right) d_{A_j,j}^{\alpha}}, \end{aligned} \tag{31}$$

where for simplicity, we define the parameters ξ_1', ξ_2' and ξ_3' as follows:

$$\xi_1' = C_1', \quad \xi_2' = -C_2', \quad \xi_3' = \sum_{i=1}^{M} d_{i,j}^{-\alpha} C_2' + \sigma_j^2/P. \tag{32}$$

By comparing (10) and (30), it can be seen that both expressions are exactly the same under the equal power allocation scenario, but with different parameters. This indicates that we can design a general network association scheme based on the evaluated SINR, which can be applicable for both TR wideband and massive MIMO systems. This characteristics is fundamentally due to the utilization of multi-path effect, where the TR wideband system is through wide band to reveal and harvest existing multiple paths, while the massive MIMO utilizes the physical massive number of antennas to create multiple independent paths. The closed-form expression of (30) can be obtained by further considering a specific beamforming scheme. Here, let us consider the beamforming scheme of MRC, then we can have the beamforming vector $\mathbf{g}_{i,j}$ as the normalized conjugate of the CSI, i.e.,

$$\mathbf{g}_{i,j} = \frac{\mathbf{h}_{i,j}^H}{\sqrt{\mathbb{E}\left[|\mathbf{h}_{i,j}|^2\right]}}. \tag{33}$$

Moreover, as aforementioned in the system model, the Rayleigh fading channel is considered. In such a case, the CSI $h_{i,j}^{\phi}$ can be regarded as a complex Gaussian random variable with zero mean and variance γ, i.e., $h_{i,j}^{\phi} \sim \mathcal{CN}(0,\gamma)$. Based on this channel model, we can derive the second and fourth moments of $h_{i,j}^{\phi}$ as follows:

$$\mathbb{E}\left[|h_{i,j}^{\phi}|^2\right] = \gamma, \tag{34}$$

$$\mathbb{E}\left[|h_{i,j}^{\phi}|^4\right] = 2\left(\mathbb{E}\left[|h_{i,j}|^2\right]\right)^2 = 2\gamma^2, \tag{35}$$

$$\mathbb{E}\left[|\mathbf{h}_{i,j}|^2\right] = \sum\nolimits_{\phi=1}^{\Phi} \mathbb{E}\left[|h_{i,j}^{\phi}|^2\right] = \Phi\gamma, \tag{36}$$

$$\mathbb{E}\left[|\mathbf{h}_{i,j}|^4\right] = \mathbb{E}\left[\left|\sum\nolimits_{\phi=1}^{\Phi}\left|h_{i,j}^{\phi}\right|^2\right|^2\right] = \Phi(\Phi+1)\gamma^2, \tag{37}$$

Then, the constants C_1' and C_2' can be calculated by

$$C_1' = \mathbb{E}\left[|\mathbf{h}_{i,j}\mathbf{g}_{i,j}|^2\right] = \frac{\mathbb{E}\left[|\mathbf{h}_{i,j}|^4\right]}{\mathbb{E}\left[|\mathbf{h}_{i,j}|^2\right]} = (\Phi+1)\gamma, \tag{38}$$

$$C_2' = \mathbb{E}\left[|\mathbf{h}_{i,j}\mathbf{g}_{i,j'}|^2\right] = \mathbb{E}\left[\left|\sum\nolimits_{\phi=1}^{\Phi} h_{i,j}^{\phi} g_{i,j'}^{\phi}\right|^2\right] \tag{39}$$

$$= \frac{\sum_{\phi=1}^{\Phi}\mathbb{E}\left[|h_{i,j}^{\phi}|^2\right]\mathbb{E}\left[|(h_{i,j'}^{\phi})^*|^2\right]}{\sum_{\phi=1}^{\Phi}\mathbb{E}\left[|h_{i,j'}^{\phi}|^2\right]} = \gamma. \tag{40}$$

Thus, we can have the parameters ξ_1', ξ_2' and ξ_3' as follows:

$$\xi_1' = (\Phi+1)\gamma, \quad \xi_2' = -\gamma, \quad \xi_3' = \sum_{i=1}^{M} d_{i,j}^{-\alpha}\gamma + \sigma_j^2/P. \tag{41}$$

Finally, by combing (30) and (40), we have obtained the SINR evaluation of the massive MIMO system. In the next section, we will propose a network association scheme for both TR wideband and massive MIMO systems, based on the effective SINR evaluation.

VI. General Network Association Protocols Design

In this section, we design a general UE sharing algorithm that can be applicable for both TR wideband and massive

MIMO systems. In the previous section, it has been shown that the SINR of TR wideband and massive MIMO systems share the exactly same expression as follows

$$\mathrm{SINR}_j = \frac{\xi_1}{\xi_2 + \xi_3 \left(\left|\mathcal{N}_{A_j}\right| + 1\right) d_{A_j,j}^{\alpha}}, \tag{42}$$

where only the parameters ξ_1, ξ_2 and ξ_3 are different for the two systems. Based on this general SINR expression, we first propose a centralized scheme with the target of maximizing all UEs' SINR, and then a distributed scheme with the target of maximizing the new arriving UE's SINR. The centralized scheme is more reasonable from the perspective of the overall network performance, but it is also associated with more computation and communication complexities. The distributed scheme is a greedy algorithm with low complexity, but only takes into account the new arrival's performance. Nevertheless, since both systems are inherent with the property of low IUI, the performance of the distributed scheme is quite similar to that of the centralized one, which will be verified in the simulation section.

A. Centralized Scheme

In practical network systems, UEs register and leave the network sequentially. Therefore, let us consider a dynamic UE arriving and then associating scenario. Suppose there are M BSs and N UEs in the network, where each BS is currently serving some existing UEs. Note that when referring to BS in this section, we will not differentiate between a TR wideband BS and a massive MIMO BS due to the similarity. Considering a new UE arrives at the network, a straightforward problem is which BS the new UE should register and associate with. The new UE should share the entire spectrum resource with all other UEs, but share the power resource only with UEs in the same BS. Apparently, the existing UEs' performance may degrade due to the power sharing and inter-user interference from the new UE. Nevertheless, the existing UEs have the priority of maintaining current BS associations as well as the satisfied quality of service (QoS), which is a common assumption in current prevailing systems like 3G and 4G.

When it comes to the centralized scheme, the new UE's association should maximize the overall system throughput, i.e., the social welfare, while given the condition that the existing UEs remain in the associated BSs and their resultant throughput can still satisfy the corresponding QoS requirement. Let us use j' to represent the existing UEs and j to represent the new UE. Thus, we can model the association problem by the following

$$\begin{aligned} &\max \sum_{j'=1}^{N} R'_{j'} + R'_j \\ &\text{s.t. } R'_j \geq R_j^{\mathrm{th}}, \quad R'_{j'} \geq R_{j'}^{\mathrm{th}} \quad \forall j', \end{aligned} \tag{43}$$

where $R'_{\cdot}$ represents the UE's expected throughput after the new arrival UE j joins the network, and $R_{\cdot}^{\mathrm{th}}$ represents the minimum QoS requirement of the UE. Since all the existing UEs are supposed to maintain their connections to the current associated BSs, the optimization problem in (42) is equivalent to the following problem

$$\max \sum_{j'=1}^{N} R'_{j'} + R'_j \Rightarrow \max \sum_{j'=1}^{N} R'_{j'} + R'_j - \sum_{j'=1}^{N} R_{j'}, \tag{44}$$

where $R_{j'}$ represents the existing UEs' expected throughput before the new UE joins the network.

Moreover, since the overall transmission power of each BS is assumed to be fixed, the expected ICI should not be affected by the new arrival UE, i.e., the new one would not impose more ICI to the UE in a different BS. Instead, the new UE only affects the performance of the UEs that share the same BS with it due to the power sharing and IUI. Suppose the new UE j accesses BS A_j, we can re-write (43) as follows:

$$\begin{aligned} &\sum_{j'=1}^{N} R'_{j'} + R'_j - \sum_{j'=1}^{N} R_{j'} \\ &\quad = R'_j + \sum_{j' \in \mathcal{N}_{A_j}} \left(R'_{j'} - R_{j'}\right) \\ &\quad = \log\left(1 + \frac{\xi_1}{\xi_2 + \xi_3 \left(\left|\mathcal{N}_{A_j}\right| + 1\right) d_{A_j,j}^{\alpha}}\right) \\ &\qquad + \sum_{j' \in \mathcal{N}_{A_j}} \left[\log\left(1 + \frac{\xi_1}{\xi_2 + \xi_{3,j'} \left(\left|\mathcal{N}_{A_j}\right| + 1\right) d_{A_j,j'}^{\alpha}}\right)\right. \\ &\qquad\qquad \left. - \log\left(1 + \frac{\xi_1}{\xi_2 + \xi_{3,j'} \left|\mathcal{N}_{A_j}\right| d_{A_j,j'}^{\alpha}}\right)\right] \\ &\quad = \log\left[\frac{\xi_1 + \xi_2 + \xi_3 \left(\left|\mathcal{N}_{A_j}\right| + 1\right) d_{A_j,j}^{\alpha}}{\xi_2 + \xi_3 \left(\left|\mathcal{N}_{A_j}\right| + 1\right) d_{A_j,j}^{\alpha}}\right. \\ &\qquad \cdot \prod_{j' \in \mathcal{N}_{A_j}} \left(\frac{\xi_1 + \xi_2 + \xi_{3,j'} \left(\left|\mathcal{N}_{A_j}\right| + 1\right) d_{A_j,j'}^{\alpha}}{\xi_2 + \xi_{3,j'} \left(\left| \quad N_{A_j}\right| + 1\right) d_{A_j,j'}^{\alpha}}\right. \\ &\qquad\qquad \left.\left. \times \frac{\xi_2 + \xi_{3,j'} \left|\mathcal{N}_{A_j}\right| d_{A_j,j'}^{\alpha}}{\xi_1 + \xi_2 + \xi_{3,j'} \left|\mathcal{N}_{A_j}\right| d_{A_j,j'}^{\alpha}}\right)\right] \\ &\quad = \log\left(\frac{\xi_1 + \xi_2 + \xi_3 \left(\left|\mathcal{N}_{A_j}\right| + 1\right) d_{A_j,j}^{\alpha}}{\xi_2 + \xi_3 \left(\left|\mathcal{N}_{A_j}\right| + 1\right) d_{A_j,j}^{\alpha}} \cdot \xi_{4,A_j}\right), \end{aligned} \tag{45}$$

where ξ_{4,A_j} is

$$\begin{aligned} \xi_{4,A_j} = &\prod_{j' \in \mathcal{N}_{A_j}} \frac{\xi_1 + \xi_2 + \xi_{3,j'} \left(\left|\mathcal{N}_{A_j}\right| + 1\right) d_{A_j,j'}^{\alpha}}{\xi_2 + \xi_{3,j'} \left(\left|\mathcal{N}_{A_j}\right| + 1\right) d_{A_j,j'}^{\alpha}} \\ &\cdot \frac{\xi_2 + \xi_{3,j'} \left|\mathcal{N}_{A_j}\right| d_{A_j,j'}^{\alpha}}{\xi_1 + \xi_2 + \xi_{3,j'} \left|\mathcal{N}_{A_j}\right| d_{A_j,j'}^{\alpha}}, \end{aligned} \tag{46}$$

representing the existing UEs' performance loss due to the admission of the new UE. Thus, the optimization problem in (42) can be transformed to the following problem

$$\begin{aligned} &\arg\max_{A_j} \frac{\xi_1 + \xi_2 + \xi_3 \left(\left|\mathcal{N}_{A_j}\right| + 1\right) d_{A_j,j}^{\alpha}}{\xi_2 + \xi_3 \left(\left|\mathcal{N}_{A_j}\right| + 1\right) d_{A_j,j}^{\alpha}} \cdot \xi_{4,A_j} \\ &\text{s.t. } R'_j \geq R_j^{\mathrm{th}}, \quad R'_{j'} \geq R_{j'}^{\mathrm{th}} \quad \forall j'. \end{aligned} \tag{47}$$

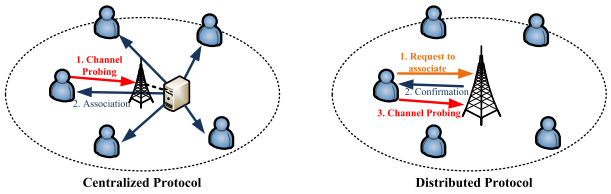

Fig. 5. Illustration of centralized and distributed protocols.

Note that there is only one variable A_j in the problem (46) and the variable A_j can only be one of the M BSs, solving the problem is as simple as a linear search.

Based on the formulation in (46), we can design a centralized network association protocol as follows, as shown in Fig. 5. When a new UE is intent to join the network, it first broadcast an impulse to all BSs, such that the BSs can obtain the CIR information as well as estimate the corresponding distance to the new UE according to the received signal strength. Then, all the BSs report those information and the load status (the number of UEs one BS is currently serving) to a central server through the backhaul, which is in charge of calculating the parameters ξ_1, ξ_2 and ξ_3 in (46) as well as the optimal BS that the new UE should access. Notice that this centralized scheme requires a central server to gather all the information from the BSs, which would inevitably incur additional communication costs and delay. In the next subsection, we will propose a distributed scheme without requiring such a central server.

B. Distributed Scheme

The distributed scheme is preferred for the scenario without a central server. Since there is no global information of the entire network in the distributed scheme, the new arrival UE has to make its own decision on which BS it should associate with. Moreover, the performance degradation of the existing UEs is also unknown to the new UE due to the limited information. Nevertheless, the BS can decide whether to admit the new UE for the sake of ensuring that the existing UEs' QoS should be guaranteed. In such a case, a new arrival UE can only make the association decision in a greedy manner, i.e., selecting the BS that can provide the highest expected throughput, which can be easily formulated by the following problem

$$\begin{aligned} & \max \ \ R_j = \log\left(1+\mathrm{SINR}_j\right) \\ \Rightarrow \ & \max \ \ \mathrm{SINR}_j = \frac{\xi_1}{\xi_2 + \xi_3\left(\left|\mathcal{N}_{A_j}\right|+1\right) d_{A_j,j}^{\alpha}}, \\ & \text{s.t. } R_j' \geq R_j^{\text{th}}, \ \ R_{j'}' \geq R_{j'}^{\text{th}}, \ \forall j', \end{aligned} \tag{48}$$

where the definition of the notations are the same with that in (42). Since the parameters ξ_1, ξ_2 and ξ_3 are constant for a specific new UE, the problem in (47) can be simplified by

$$\begin{aligned} & \arg\min_{A_j} \ \ \left(\left|\mathcal{N}_{A_j}\right|+1\right) d_{A_j,j}^{\alpha} \\ & \text{s.t. } R_j' \geq R_j^{\text{th}}, \ \ R_{j'}' \geq R_{j'}^{\text{th}} \ \ \forall j'. \end{aligned} \tag{49}$$

Similarly, solving the problem in (48) is also a simple linear search. A toy example is for two BSs case: when the load of each BS is given, i.e., the number of existing UEs in each BS N_1 and N_2, the UE can just compare the distance according to the following rule to make the association decision

$$\frac{d_{1,j}}{d_{2,j}} \gtrless \left(\frac{|\mathcal{N}_2|+1}{|\mathcal{N}_1|+1}\right)^{1/\alpha}. \tag{50}$$

As a matter of fact, due to the small IUI in TR wideband and massive MIMO systems, the social welfare of the distributed association protocol is quite similar to that of the centralized protocol, which will be verified in the simulation section.

Based on the formulation in (48), we can design a distributed network association protocol as follows, as shown in Fig. 5. The BSs periodically broadcast the beacon signals to the network, including its ID information as well as the current load status, i.e., the number of existing UEs in it. When a new UE is intent to join the network, it can receive beacon signals from the neighboring BSs. The distance between the new UE and the BSs can be roughly estimated by the signal streghth and the path loss model. Thus, by calculation (48) with the distance and load information, the new UE can determine a priority list of BSs from the high SINR to the low one. Then, the new UE sends a request-to-access packet to the first BS on the list. When a BS receives a request, it would check the constraints in (48) to make sure the existing UEs' QoS requirement can be still satisfied. If this can be confirmed, the BS sends a confirmation to the new UE to establish connections. If no confirmation is received within a certain period, the UE would send a request to the second BS on the priority list, so on and so forth.

TABLE I
SIMULATION PARAMETERS

Parameters	TR wideband	Massive MIMO
Bandwidth	1 GHz	40 MHz
Number of BSs	$M=3$	$M=3$
Number of antennas	1	100
SNR	20 dB	20 dB
Path loss	$\alpha=4$	$\alpha=4$
Back off factor	$D=16$	$D=0$
Sampling period	$T_s=1$ns	$T_s=1$ns
Channel length	$L=256$	$L=1$

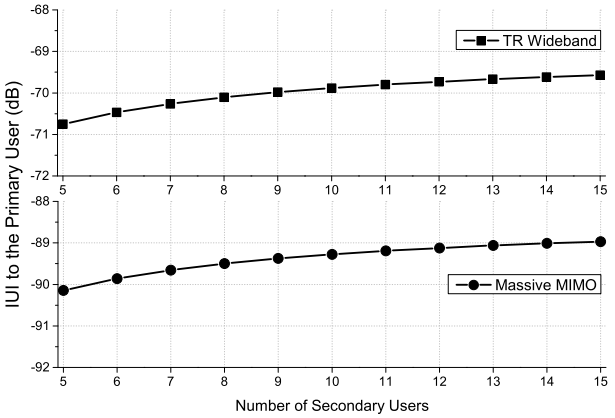

Fig. 6. Inter-User interference in both systems.

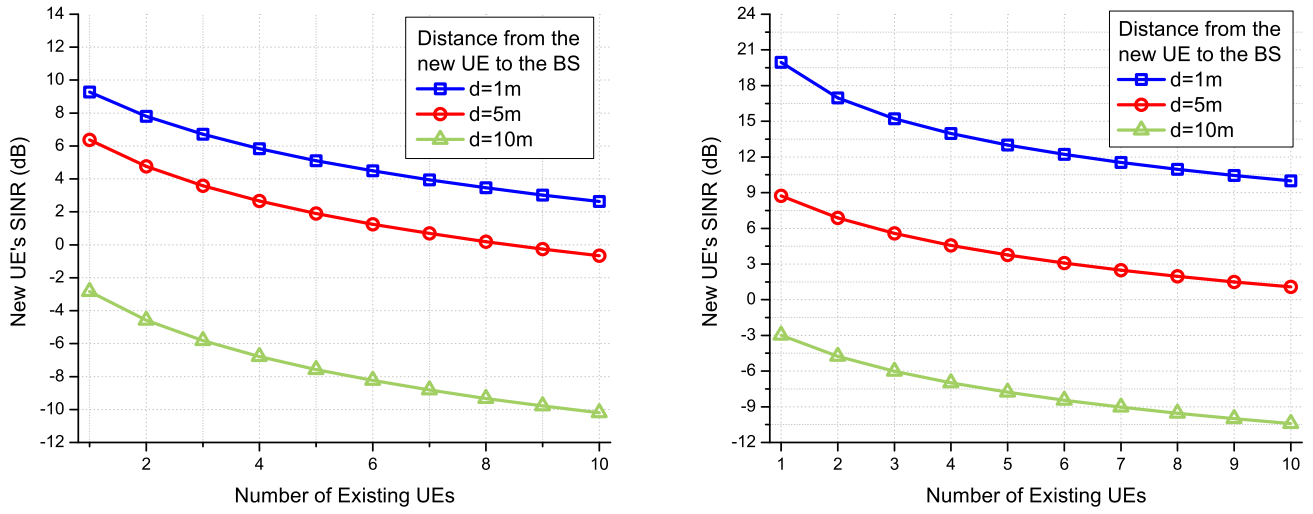

(a) TR wideband system.

(b) Massive MIMO system.

Fig. 7. SINR performance of the new UE. (a) TR wideband system. (b) Massive MIMO system.

VII. Simulation Results

In this section, we conduct simulation to evaluate the performance of the proposed spatial spectrum sharing framework, where both TR wideband systems and massive MIMO systems are considered. For the TR wideband system, we consider the broadband with frequency bandwidth that typically ranges from hundreds of MHz to several GHz, which is much wider than those narrow-band systems specified in 3GPP/4G. In the rich scattering environment, such a broadband system can differentiate rich independent multiple paths, which can help create super-high spatial focusing gain as shown in Fig. 3-(a). On the other hand, for the massive MIMO system, we still consider the traditional narrow-band setting with frequency bandwidth of $20-40$ MHz, but with massive number of antennas as to one hundred. Those massive antennas can provide highly independent channel statistics of different locations and also help create super-high spatial focusing gain as shown in Fig. 3-(b). Table I summarizes the simulation setting of the two systems. For the TR wideband system with 1 GHz bandwidth and the sampling period $T_s = 1$ ns, the channel length is typically $L = 256$ and the root mean square delay spread is typically $\sigma_T = 128T_s$, according to the IEEE 802.15.4a outdoor non-line-of-sight channels. While for the massive MIMO system, OFDM technology is adopted for each antenna and each subcarrier is considered to be with channel length $L = 1$.

Let us first validate the spatial spectrum sharing performance by simulating a BS serving both primary users and secondary users. We consider the scenario that one primary user and 5 secondary users are currently served by one BS, and then 10 more secondary users are sequentially admitted by the same BS sharing the entire spectrum with the existing users. The distance between the primary user and the BS is set as 15 meters, while the locations of the secondary users are randomly generated. Fig. 6 shows the IUI to the primary user when different number of secondary users join the BS, where the y-axis is IUI/Noise in dB. We can see that the IUI

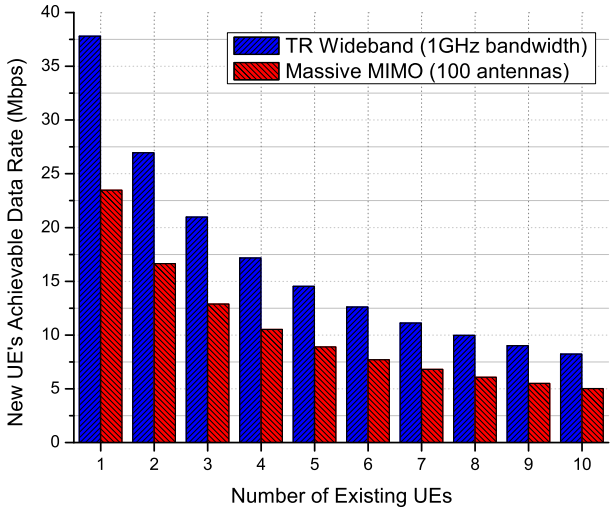

Fig. 8. Achievable Data Rate of the new UE in both systems.

to the primary user increases slightly when more and more secondary users are admitted, i.e., approximately only 1 dB loss from 5 to 10 existing secondary users. Therefore, the spatial focusing effect can greatly decrease the IUI and enable the co-existence of primary users and secondary users on the entire spectrum.

Then, let us investigate the SINR performance of the new arrival UE in both systems, as shown in Fig. 7 under different numbers of existing UEs in the associated BS, i.e., from 1 UE to 10 UEs. The distance between the new UE and the associated BS is configured as 1m, 5m and 10m, respectively, which are corresponding to the three curves in each sub-figure of Fig. 7. The distances between the new UE and the other two interference BSs are set as 20m. Generally, the results in both sub-figures show that when the number of existing UEs increases, i.e., the associated BS becomes more and more crowded, the SINR of each individual UE decreases due to the power sharing and IUI. Meanwhile,

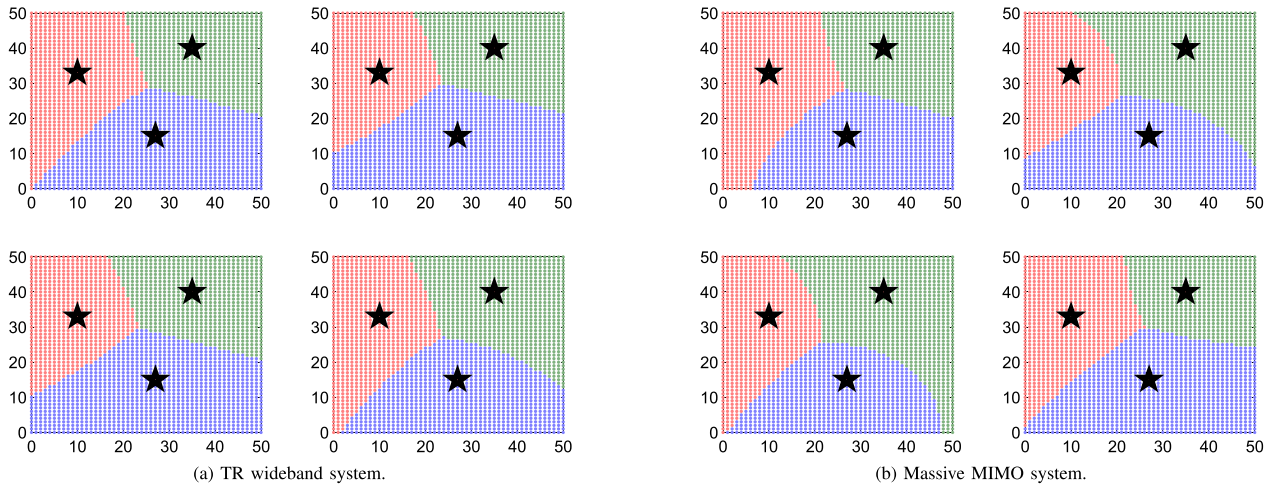

(a) TR wideband system. (b) Massive MIMO system.

Fig. 9. Network association illustration. (a) TR wideband system. (b) Massive MIMO system.

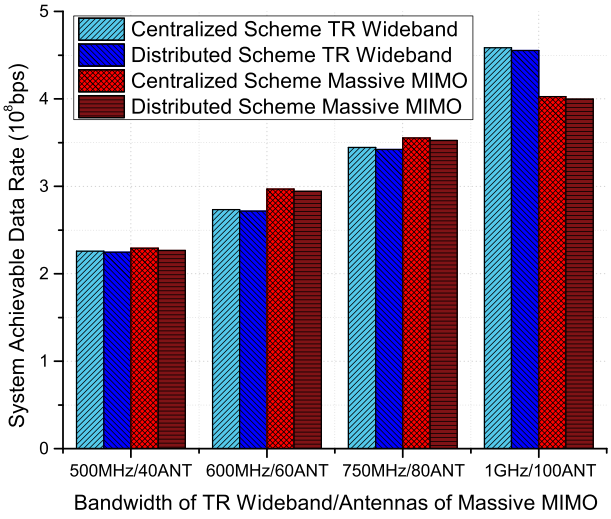

Fig. 10. Network association performance in both systems.

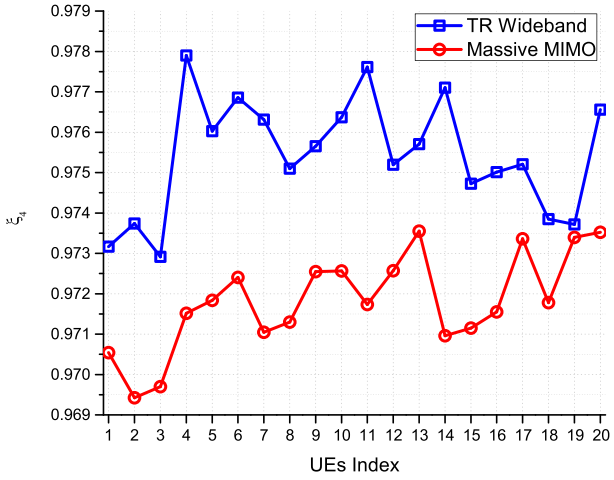

Fig. 11. Value of ξ_4 in both systems.

the farther distance between the new UE and the associated BS can also lead to decreased SINR due to the path loss. Moreover, we also show the numerical achievable data rate of the new UE in Fig. 8. Note that the TR wideband data rate is calculated by $B/D\log(1+\text{SINR})$ and the massive MIMO data rate is calculated by $B\log(1+\text{SINR})$. It can be seen that both systems can achieve high throughput either by wide bandwidth for TR wideband or by a large number of antennas for massive MIMO.

Based on the SINR performance evaluation, we further simulate the new UE's association status and show the results of both systems in Fig. 9, where a two-dimensional plane with an area of 50m×50m is considered. The pentagrams in each area represent three BSs, whose locations are [10, 33], [27, 15], and [35, 40], respectively. For each sub-figure, we first generate 20 existing UEs with random locations and simply associate each UE with the corresponding BS. Then, we consider each location in the area as a new arrival UE's location to check which BS should cover this location. The color in the figure means the region that should be covered by the center BS when a new UE appears. Additionally, for each system, we simulate four different association status under different settings of existing UEs. We can see that the existing load of the BSs affects the new UE's association to a large extent. While an interesting phenomenon is that, due to the spatial focusing effect, the boundary between two BSs may vary under different settings of the locations and number of existing UEs in the network. Therefore, in the 5G networks, the traditional fixed boundary between two cells, which is purely determined by the locations and distances, may not hold. On one hand, the spatial focusing gain discussed in Section III can help extend the coverage of one BS. On the other hand, the more UEs share one BS can decrease the power resource of each individual UE and thus lead to the shrinking of the coverage.

Finally, let us evaluate the proposed centralized and distributed network association protocols. In this simulation, the locations of BSs and the 50m×50m plane are the same as that in Fig. 9. In each simulation run, 20 UEs are randomly generated within the plane. Once a new UE is generated, the proposed association protocols are utilized to determine whether the BS admitting the new UE. We conduct 1000 independent runs and calculate the average network throughput of both protocols shown in Fig. 10. For the TR wideband

system, the protocols are evaluated under different bandwidths from 500MHz to 1GHz; while for the massive MIMO system, the protocols are evaluated under different numbers of antennas from 40 to 100. Surprisingly, the performance of the distributed protocol, which is expected to be worse than the optimal centralized protocol, is indeed similar to that of the centralized one. This phenomenon can be explained by an important parameter ξ_4 defined in (45), which represents the existing UEs' performance loss due to the new UE's association. From (45), we can see that when the number of existing UEs $\left|\mathcal{N}_{A_j}\right|$ is small, the parameters ξ_2 and ξ_3 representing the combination of ISI and IUI are far less than the parameter ξ_1 representing the signal power due to the spatial focusing gain. In such a case, ξ_4 should be approximately equal to 1. While on the other hand, when the number of existing UEs $\left|\mathcal{N}_{A_j}\right|$ is sufficiently large, ξ_4 would approach 1 again. To further validate this, we plot the value of ξ_4 under different numbers of UEs in both systems in Fig. 11, from which it can be seen that ξ_4 is always approximately 1. Knowing the characteristic of $\xi_4 \approx 1$, let us then review the objective functions of both protocols as follows:

Centralized Scheme:

$$\arg\max_{A_j} \frac{\xi_1 + \xi_2 + \xi_3 \left(\left|\mathcal{N}_{A_j}\right| + 1\right) d_{A_j,j}^{\alpha}}{\xi_2 + \xi_3 \left(\left|\mathcal{N}_{A_j}\right| + 1\right) d_{A_j,j}^{\alpha}} \cdot \xi_{4,A_j}, \tag{51}$$

Distributed Scheme:

$$\arg\min_{A_j} \left(\left|\mathcal{N}_{A_j}\right| + 1\right) d_{A_j,j}^{\alpha}. \tag{52}$$

We can see that the only parameter that determines the difference of these two schemes is ξ_4. When $\xi_4 \approx 1$, the centralized scheme becomes

$$\begin{aligned} &\max_{A_j} \frac{\xi_1 + \xi_2 + \xi_3 \left(\left|\mathcal{N}_{A_j}\right| + 1\right) d_{A_j,j}^{\alpha}}{\xi_2 + \xi_3 \left(\left|\mathcal{N}_{A_j}\right| + 1\right) d_{A_j,j}^{\alpha}} \\ &\Rightarrow \max_{A_j} 1 + \frac{\xi_1}{\xi_2 + \xi_3 \left(\left|\mathcal{N}_{A_j}\right| + 1\right) d_{A_j,j}^{\alpha}} \\ &\Rightarrow \min_{A_j} \left(\left|\mathcal{N}_{A_j}\right| + 1\right) d_{A_j,j}^{\alpha}, \end{aligned} \tag{53}$$

which leads to the equivalence of these two schemes. Again, due to the spatial focusing effect which brings the benefit of rather small interference among UEs, the distributed protocol with low complexity can be practically adopted in both TR wideband and massive MIMO systems.

VIII. Conclusions

In this paper, we proposed a general spatial spectrum sharing architecture based on the spatial focusing characteristic in both TR wideband and massive MIMO systems. The spatial focusing phenomenon was first shown by simulation results, as well as real-world experiment. Relying on this phenomenon, we analyzed the SINR performance of concurrently spatial spectrum sharing for both TR wideband and massive MIMO systems. It turned out to be that the SINR of both systems shared exactly the same expression under the equal power allocation scenario, which motivated us to design a general network association protocol. The centralized and distributed association schemes were designed, while the performance of the distributed scheme was quite similar to that of the centralized one, due to the benefit of rather small IUI brought by the spatial focusing effect. Since the realization of the spatial focusing effect relies on the accurate CSI of all users, the major challenge of the proposed scheme is how to simultaneously collect the users' CSI especially when the number of users is considerable. To summarize, with the trends of wider bandwidth and larger scale of antennas, spatial focusing effect becomes the uniqueness of the next generation networks.

In the future, this effect can be a bridge that separates the physical layer and MAC layer design, where the physical layer design should focus on how to strengthen this focusing effect in order to alleviate interference, while the MAC layer design should concentrate on how to utilize this effect to accommodate more users. Therefore, more MAC layer issues should be re-investigated when the spatial focusing effect is taken into account, e.g., the admission control, the handover, as well as the security issue. Meanwhile, the other channel models can be considered, for example Winner II channel model, in which there is a correlation between different paths.

References

[1] C. Jiang, Y. Chen, K. J. R. Liu, and Y. Ren, "Renewal-theoretical dynamic spectrum access in cognitive radio network with unknown primary behavior," *IEEE J. Sel. Areas Commun.*, vol. 31, no. 3, pp. 406–416, Mar. 2013.

[2] F. R. V. Guimaraes, D. B. Da Costa, T. A. Tsiftsis, C. C. Cavalcante, G. K. Karagiannidis, and F. Rafael, "Multiuser and multirelay cognitive radio networks under spectrum-sharing constraints," *IEEE Trans. Veh. Technol.*, vol. 63, no. 1, pp. 433–439, Jan. 2014.

[3] J. J. Meng, W. Yin, H. Li, E. Hossain, and Z. Han, "Collaborative spectrum sensing from sparse observations in cognitive radio networks," *IEEE J. Sel. Areas Commun.*, vol. 29, no. 2, pp. 327–337, Feb. 2011.

[4] Q. Wu, G. Ding, J. Wang, and Y. D. Yao, "Spatial-temporal opportunity detection for spectrum-heterogeneous cognitive radio networks: Two-dimensional sensing," *IEEE Trans. Wireless Commun.*, vol. 12, no. 2, pp. 516–526, Feb. 2013.

[5] B. Wang, Y. Wu, F. Han, Y.-H. Yang, and K. J. R. Liu, "Green wireless communications: A time-reversal paradigm," *IEEE J. Sel. Areas Commun.*, vol. 29, no. 8, pp. 1698–1710, Sep. 2011.

[6] Y. Chen, B. Wang, Y. Han, H.-Q. Lai, Z. Safar, and K. J. R. Liu, "Why time-reversal for future 5G wireless?" *IEEE Signal Process. Mag.*, vol. 33, no. 2, pp. 17–26, Mar. 2016.

[7] F. Rusek *et al.*, "Scaling up MIMO: Opportunities and challenges with very large arrays," *IEEE Signal Process. Mag.*, vol. 30, no. 1, pp. 40–60, Jan. 2013.

[8] C. Oestges, A. D. Kim, G. Papanicolaou, and A. J. Paulraj, "Characterization of space-time focusing in time-reversed random fields," *IEEE Trans. Antennas Propag.*, vol. 53, no. 1, pp. 283–293, Jan. 2005.

[9] A. M. Akhtar, X. Wang, and L. Hanzo, "Synergistic spectrum sharing in 5G HetNets: A harmonized SDN-enabled approach," *IEEE Commun. Mag.*, vol. 54, no. 1, pp. 40–47, Jan. 2016.

[10] G. Ding *et al.*, "On the limits of predictability in real-world radio spectrum state dynamics: From entropy theory to 5G spectrum sharing," *IEEE Commun. Mag.*, vol. 54, no. 7, pp. 178–183, Jul. 2015.

[11] B. Li, S. Li, A. Nallanathan, and C. Zhao, "Deep sensing for future spectrum and location awareness 5G communications," *IEEE J. Sel. Areas Commun.*, vol. 33, no. 7, pp. 1331–1344, Jul. 2015.

[12] J. Mitola *et al.*, "Accelerating 5G QoE via public-private spectrum sharing," *IEEE Commun. Mag.*, vol. 52, no. 5, pp. 77–85, May 2014.

[13] D. W. K. Ng, M. Breiling, C. Rohde, F. Burkhardt, and R. Schober, "Energy-efficient 5G outdoor-to-indoor communication: Sudas over licensed and unlicensed spectrum," *IEEE Trans. Wireless Commun.*, vol. 15, no. 5, pp. 3170–3186, May 2016.

[14] B. Singh *et al.*, "Coordination protocol for inter-operator spectrum sharing in co-primary 5G small cell networks," *IEEE Commun. Mag.*, vol. 53, no. 7, pp. 34–40, Jul. 2015.

[15] C. Jiang, Y. Chen, Y. Gao, and K. J. R. Liu, "Joint spectrum sensing and access evolutionary game in cognitive radio networks," *IEEE Trans. Wireless Commun.*, vol. 12, no. 5, pp. 2470–2483, May 2013.
[16] C. Jiang, Y. Chen, and K. J. R. Liu, "Multi-channel sensing and access game: Bayesian social learning with negative network externality," *IEEE Trans. Wireless Commun.*, vol. 13, no. 4, pp. 2176–2188, Apr. 2014.
[17] S. Singh, R. Mudumbai, and U. Madhow, "Interference analysis for highly directional 60-GHZ mesh networks: The case for rethinking medium access control," *IEEE/ACM Trans. Netw.*, vol. 19, no. 5, pp. 1513–1527, May 2011.
[18] H. Shokri-Ghadikolaei, C. Fischione, G. Fodor, P. Popovski, and M. Zorzi, "Millimeter wave cellular networks: A MAC layer perspective," *IEEE Trans. Wireless Commun.*, vol. 63, no. 10, pp. 3437–3458, Oct. 2015.
[19] T. Bai and R. W. Heath, Jr., "Coverage and rate analysis for millimeter-wave cellular networks," *IEEE Trans. Wireless Commun.*, vol. 14, no. 2, pp. 1100–1114, Feb. 2015.
[20] G. Athanasiou, P. C. Weeraddana, C. Fischione, and L. Tassiulas, "Optimizing client association for load balancing and fairness in millimeter-wave wireless networks," *IEEE/ACM Trans. Netw.*, vol. 23, no. 3, pp. 836–850, Jun. 2015.
[21] J. Garcia-Rois *et al.*, "On the analysis of scheduling in dynamic duplex multihop mm-wave cellular systems," *IEEE Trans. Wireless Commun.*, vol. 14, no. 11, pp. 6028–6042, Nov. 2015.
[22] P. Wang, W. Song, D. Niyato, and Y. Xiao, "QoS-aware cell association in 5G heterogeneous networks with massive MIMO," *IEEE Netw.*, vol. 29, no. 6, pp. 76–82, Nov./Dec. 2015.
[23] C. Jiang, Y. Chen, K. J. R. Liu, and Y. Ren, "Network economics in cognitive networks," *IEEE Commun. Mag.*, vol. 53, no. 5, pp. 75–81, May 2015.
[24] C. Jiang, Y. Chen, Y.-H. Yang, C.-Y. Wang, and K. J. R. Liu, "Dynamic chinese restaurant game: Theory and application to cognitive radio networks," *IEEE Trans. Wireless Commun.*, vol. 13, no. 4, pp. 1960–1973, Apr. 2014.
[25] D. Bethanabhotla, O. Y. Bursalioglu, H. C. Papadopoulos, and G. Caire, "Optimal user-cell association for massive mimo wireless networks," *IEEE Trans. Wirelss Commun.*, vol. 15, no. 3, pp. 1835–1850, Mar. 2016.
[26] D. Liu, L. Wang, Y. Chen, T. Zhang, K. Chai, and M. Elkashlan, "Distributed energy efficient fair user association in massive MIMO enabled HetNets," *IEEE Commun. Lett.*, vol. 19, no. 10, pp. 1770–1773, Oct. 2015.
[27] N. Wang, E. Hossain, and V. K. Bhargava, "Joint downlink cell association and bandwidth allocation for wireless backhauling in two-tier hetnets with large-scale antenna arrays," *IEEE Trans. Wirelss Commun.*, vol. 15, no. 5, pp. 3251–3268, May 2016.
[28] F. Han, Y. H. Yang, B. Wang, Y. Wu, and K. J. R. Liu, "Time-reversal division multiple access over multi-path channels," *IEEE Trans. Commun.*, vol. 60, no. 7, pp. 1953–1965, Jul. 2012.
[29] Y. H. Yang, B. Wang, W. S. Lin, and K. J. R. Liu, "Near-optimal waveform design for sum rate optimization in time-reversal multiuser downlink systems," *IEEE Trans. Wireless Commun.*, vol. 12, no. 1, pp. 346–357, Jan. 2013.
[30] Q. Y. Xu, Y. Chen, and K. J. R. Liu, "Combating strong-weak spatial-temporal resonances in time-reversal uplinks," *IEEE Trans. Wirelss Commun.*, vol. 15, no. 1, pp. 1953–1965, Jan. 2016.
[31] F. Han and K. J. R. Liu, "A multi–user TRDMA uplink system with 2D parallel interference cancellation," *IEEE Trans. Commun.*, vol. 62, no. 3, pp. 1011–1022, Mar. 2014.
[32] Y.-H. Yang and K. J. R. Liu, "Waveform design with interference pre-cancellation beyond time-reversal systems," *IEEE Trans. Wireless Commun.*, vol. 15, no. 5, pp. 3643–3654, May 2016.
[33] H. Q. Ngo, E. G. Larsson, and T. L. Marzetta, "Energy and spectral efficiency of very large multiuser MIMO systems," *IEEE Trans. Commun.*, vol. 61, no. 4, pp. 1436–1449, Apr. 2013.
[34] S. Jin, X. Wang, Z. Li, K.-K. Wong, Y. Huang, and X. Tang, "On massive MIMO zero-forcing transceiver using time-shifted pilots," *IEEE Trans. Veh. Technol.*, vol. 65, no. 1, pp. 59–74, Jan. 2016.
[35] T. Cui, F. Gao, T. Ho, and A. Nallanathan, "Distributed space-time coding for two-way wireless relay networks," *IEEE Trans. Signal Process.*, vol. 57, no. 2, pp. 658–671, Feb. 2009.
[36] F. Gao, R. Zhang, and Y.-C. Liang, "Optimal channel estimation and training design for two-way relay networks," *IEEE Trans. Commun.*, vol. 57, no. 10, pp. 3024–3033, Oct. 2009.
[37] M. R. McKay, I. B. Collings, and A. M. Tulino, "Achievable sum rate of MIMO MMSE receivers: A general analytic framework," *IEEE Trans. Inf. Theory*, vol. 56, no. 1, pp. 396–410, Jan. 2010.
[38] F. Gao, T. Cui, and A. Nallanathan, "On channel estimation and optimal training design for amplify and forward relay networks," *IEEE Trans. Wireless Commun.*, vol. 7, no. 5, pp. 1907–1916, May 2008.
[39] M. Emami, M. Vu, J. Hansen, A. J. Paulraj, and G. Papanicolaou, "Matched filtering with rate back-off for low complexity communications in very large delay spread channels," in *Proc. 38th Asilomar Conf. Signals, Syst. Comput. (ACSSC)*, vol. 1. Nov. 2004, pp. 218–222.
[40] P. H. Moose, "A technique for orthogonal frequency division multiplexing frequency offset correction," *IEEE Trans. Commun.*, vol. 42, no. 10, pp. 2908–2914, Oct. 1994.
[41] J. Lee, H.-L. Lou, D. Toumpakaris, and J. M. Cioff, "Snr analysis of ofdm systems in the presence of carrier frequency offset for fading channels," *IEEE Trans. Wirelss Commun.*, vol. 5, no. 12, pp. 3360–3364, Dec. 2006.

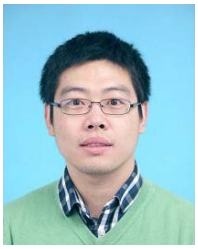

Chunxiao Jiang (S'09–M'13–SM'15) received the B.S. degree (Hons.) in information engineering from Beihang University, Beijing, China, in 2008, and the Ph.D. degree (Hons.) in electronic engineering from Tsinghua University, Beijing, in 2013. He is currently an Assistant Research Fellow with the Tsinghua Space Center, Tsinghua University. His research interests include application of game theory, optimization, and statistical theories to communication, networking, signal processing, and resource allocation problems, in particular space information networks, heterogeneous networks, social networks, and big data privacy. He was a recipient of the Best Paper Award from the IEEE GLOBECOM in 2013, the Best Student Paper Award from the IEEE GlobalSIP in 2015, the Distinguished Dissertation Award from the Chinese Association for Artificial Intelligence in 2014, and the Tsinghua Outstanding Postdoc Fellow Award (only ten winners each year) in 2015.

Beibei Wang (SM'15) received the B.S. degree (Hons.) in electrical engineering from the University of Science and Technology of China, Hefei, China, in 2004, and the Ph.D. degree in electrical engineering from the University of Maryland at College Park, College Park, MD, USA, in 2009. She was with the University of Maryland at College Park as a Research Associate from 2009 to 2010, and Qualcomm Research and Development from 2010 to 2014. Since 2015, she has been with Origin Wireless, Inc., as a Principal Technologist. She has co-authored *Cognitive Radio Networking and Security: A Game-Theoretic View* (Cambridge University Press, 2010). Her research interests include wireless communications and signal processing. She received the Graduate School Fellowship, the Future Faculty Fellowship, and the Dean's Doctoral Research Award from the University of Maryland at College Park and the Overview Paper Award from the IEEE Signal Processing Society in 2015.

Yi Han received the B.S. degree (Hons.) in electrical engineering from Zhejiang University, Hangzhou, China, in 2011, and the Ph.D. degree from the Department of Electrical and Computer Engineering, University of Maryland at College Park, College Park, MD, USA, in 2016. He is currently the Wireless Architect with Origin Wireless, Inc.. His research interests include wireless communication and signal processing.

Dr. Han was a recipient of the Class A Scholarship from the Chu Kochen Honors College, Zhejiang University, in 2008. He was also a recipient of the Best Student Paper Award of the IEEE ICASSP in 2016.

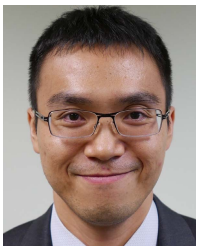

Zhung-Han Wu (S'14) received the B.S. and M.S. degrees in electrical engineering from National Taiwan University, Taipei, Taiwan, in 2008 and 2010, respectively, and the Ph.D. degree in electrical engineering from the University of Maryland at College Park, College Park, MD, USA, in 2016. He is currently with Origin Wireless, Inc., where he develops cloud-based smart radio algorithms and solutions for a wide variety of applications, including indoor positioning, tracking, and security monitoring. He received the A. James Clark School of Engineering Distinguished Graduate Fellowship in 2011 and was recognized as a Distinguished Teaching Assistant of the University of Maryland at College Park in 2013.

K. J. Ray Liu (F'03) was a Distinguished Scholar-Teacher with the University of Maryland at College Park, College Park, MD, USA, in 2007, where he is currently a Christine Kim Eminent Professor of Information Technology. He leads the Maryland Signals and Information Group conducting research encompassing broad areas of information and communications technology with recent focus on smart radios for smart life.

Dr. Liu is a member of the IEEE Board of Directors. He is a fellow of the AAAS. He was a recipient of the 2016 IEEE Leon K. Kirchmayer Technical Field Award on graduate teaching and mentoring, the IEEE Signal Processing Society 2014 Society Award, and the IEEE Signal Processing Society 2009 Technical Achievement Award. He also received teaching and research recognitions from the University of Maryland at College Park, including the university-level Invention of the Year Award; and the college level Poole and Kent Senior Faculty Teaching Award, the Outstanding Faculty Research Award, and the Outstanding Faculty Service Award, all from the A. James Clark School of Engineering. He was recognized by Thomson Reuters as a Highly Cited Researcher. He was the President of the IEEE Signal Processing Society, where he has served as a Vice President of Publications and the Board of Governors. He has also served as the Editor-in-Chief of the *IEEE Signal Processing Magazine*.